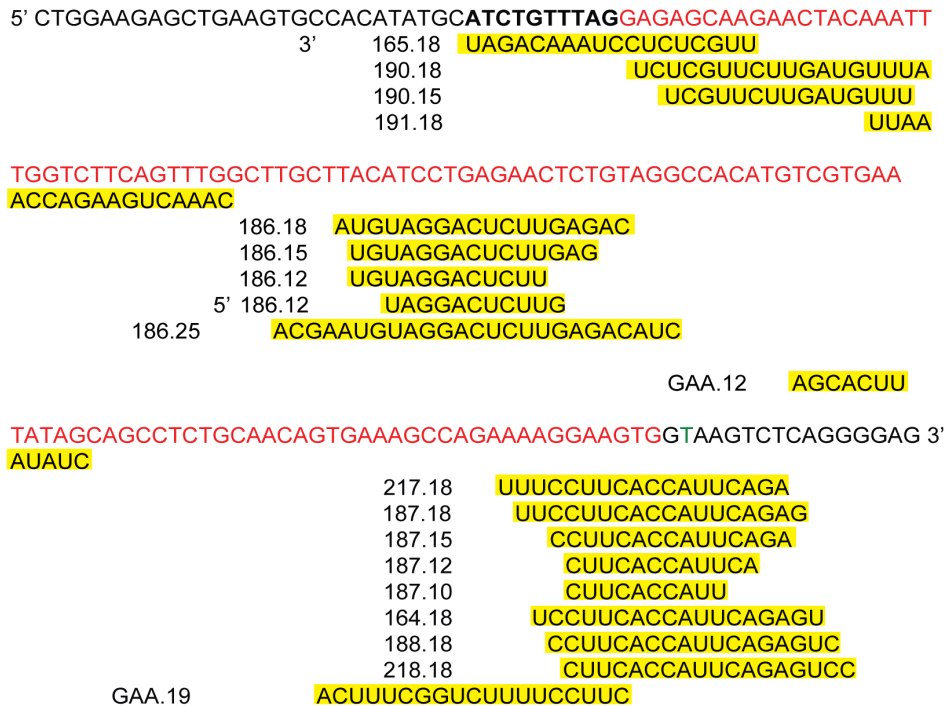
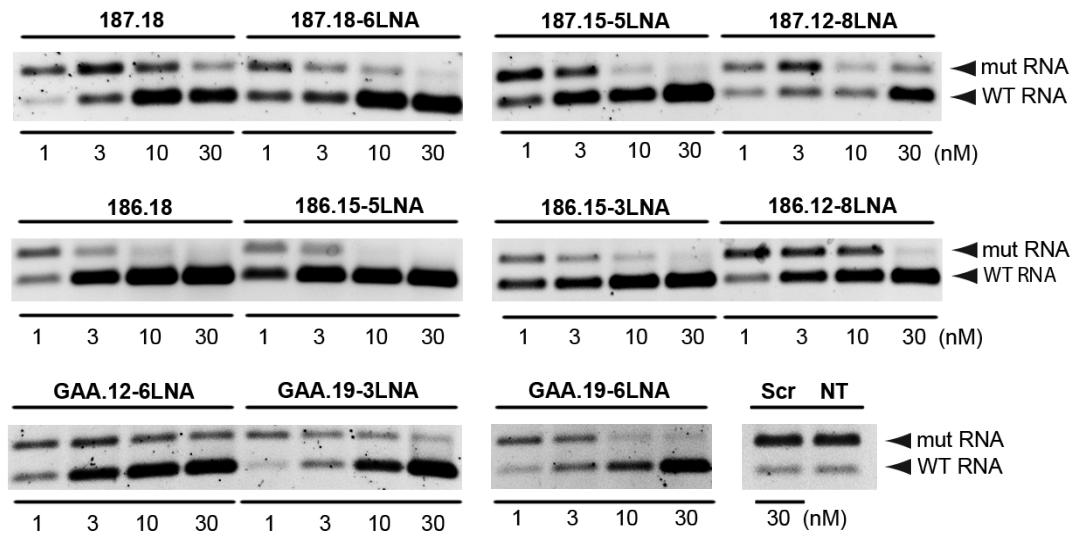


SUPPLEMENTAL FIGURES AND FIGURE LEGENDS

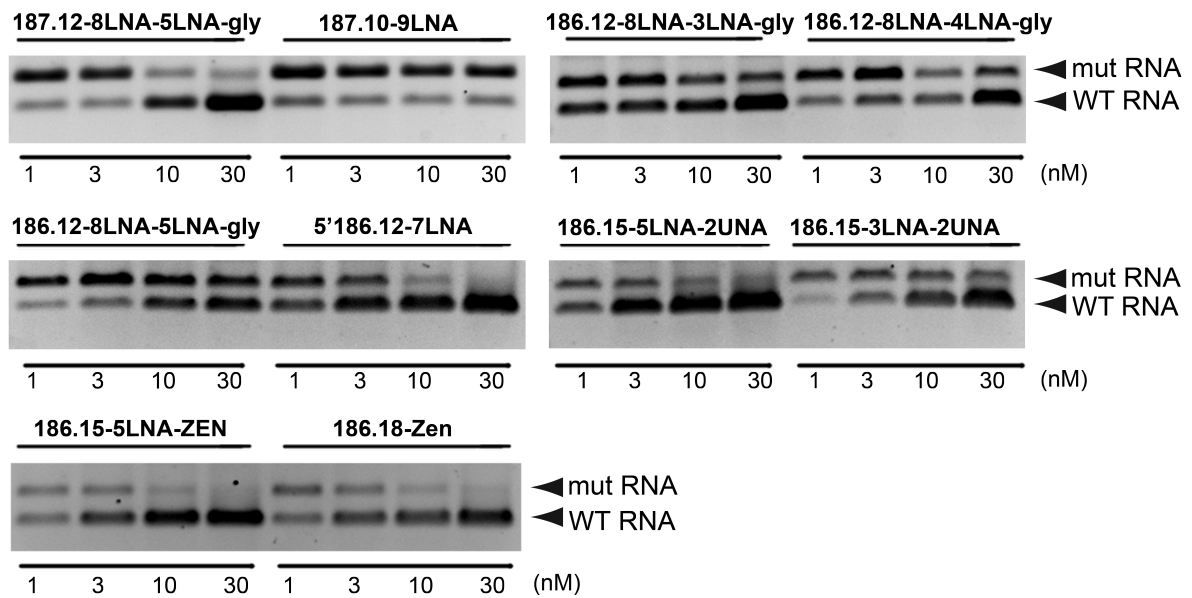
Schematics of SCOs



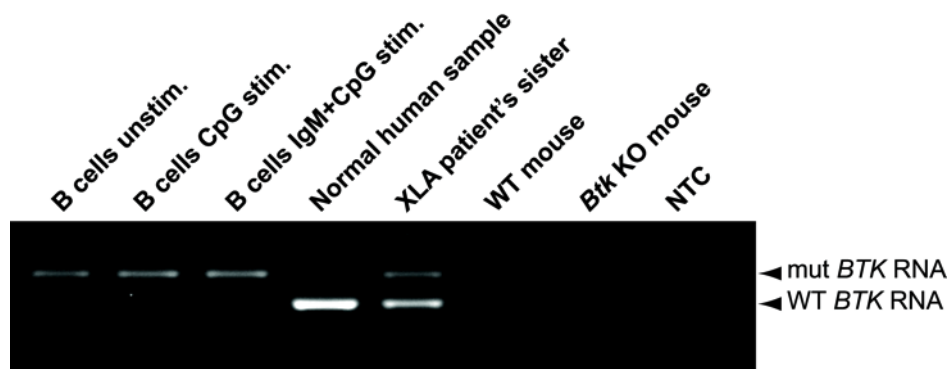
Supplemental Figure 1. Schematic drawing of the *BTK* sequence and the tested SCOs. The mutation (A to T: nucleotide in green) causes the aberrant splicing by creating a novel 5' splice-site. This leads to activation of an upstream cryptic 3' splice-site and to the inclusion of a pseudoexon (sequence in red) is depicted. In yellow are the SCOs designed to target the pseudoexon 3' and 5' splice-sites and putative exonic splicing-enhancers (ESEs). The modifications of these SCOs are indicated in Table 1. Note that SCOs 191.18 and GAA.12 are interrupted in the figure.



Supplemental Figure 2. Splice-correction-induced up-regulation of reporter mini-gene activity using further modified SCOs. Efficacy of modified SCOs from the 186-, 187- and GAA- series following transfection at low doses as measured by the restoration of *BTK* mini-gene. A concentration of 30 nM was used for the scrambled control SCO (Scr) (Table 1). A representative gel from two independent experiments is shown. NT: non-treated cells.

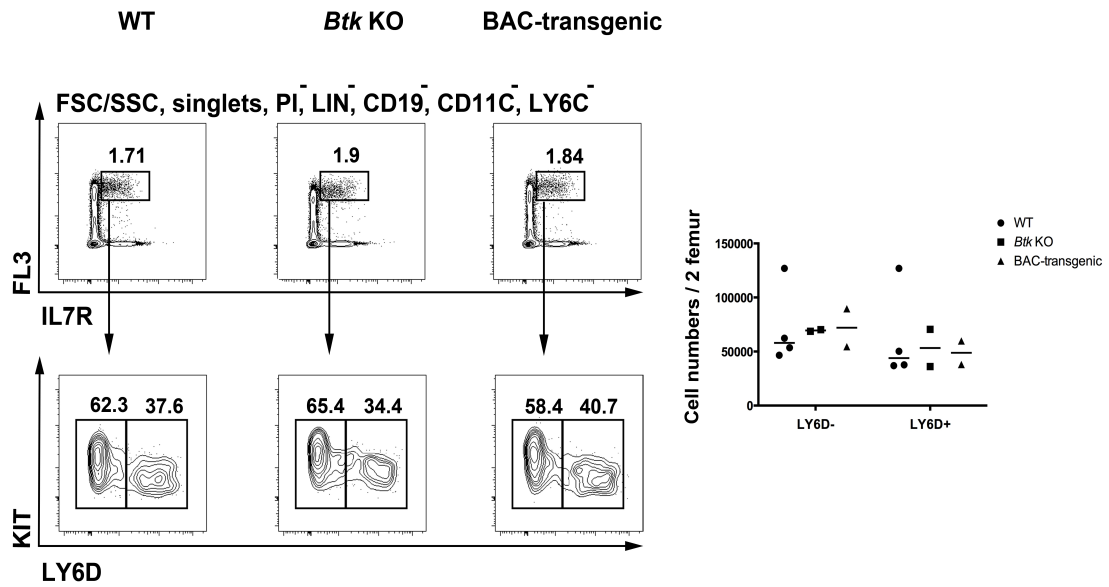


Supplemental Figure 3. Semi-quantitative RT-PCR identifying splice-correction in the mini-gene reporter cell line. Modified SCOs from the 186- and 187-series were compared by transfection at low doses. A representative gel from two independent experiments is shown.

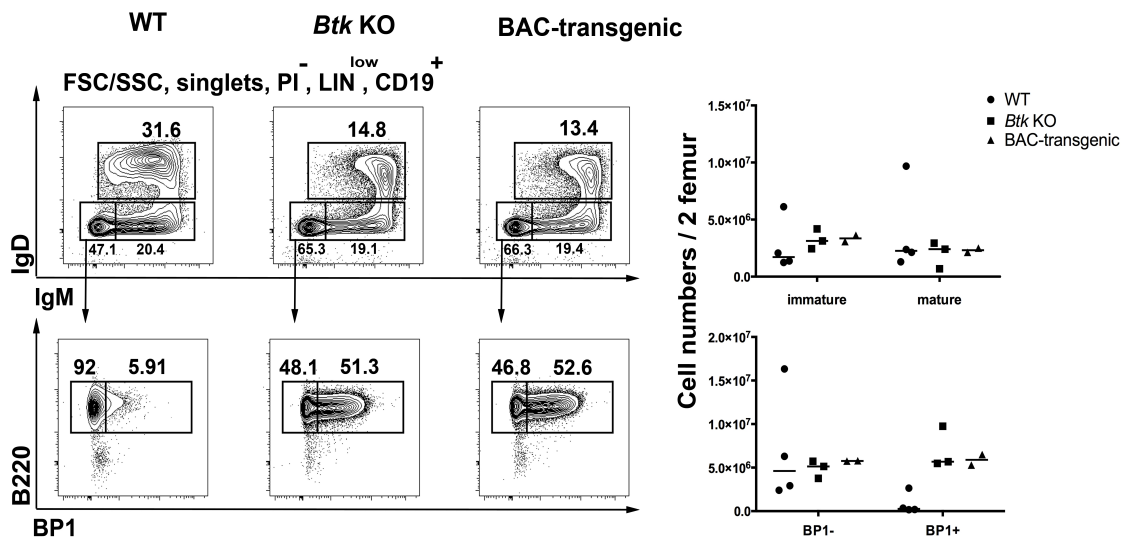


Supplemental Figure 4. Selective detection of human *BTK* mRNA in a human BAC-transgenic mouse model. RT-PCR of total RNA isolated from splenic B cells of BAC-transgenic, WT, or *Btk* KO mice, or from blood samples of a healthy control subject or a healthy carrier (XLA patient's sister). Two of the B cell samples were stimulated with CpG ON only or CpG ON together with anti-IgM in order to promote survival. The primer set was designed to only detect human *BTK* RNA, i.e. only human BAC-transgenics will generate amplicons by this assay. Since the disorder is X-linked, a healthy female carrier (here the patient's sister) will have two copies of the gene, one mutated and one normal, yielding both the aberrant and the correct mRNA species from a peripheral blood sample containing polyclonal BTK-expressing hematopoietic cells. NTC: non-treated water control.

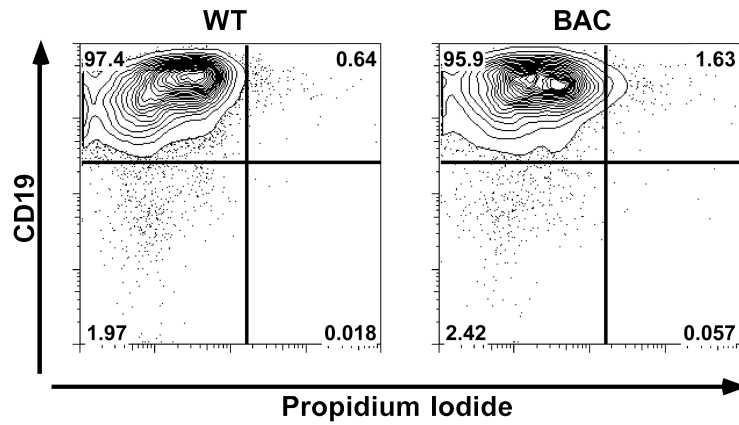
A



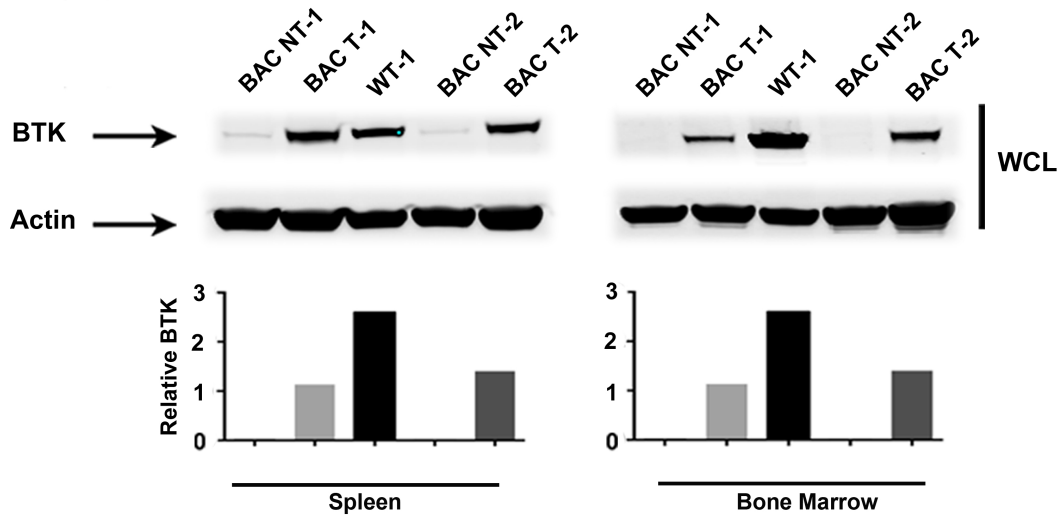
B



Supplemental Figure 5. Flow cytometric analysis showing CLPs (common lymphoid progenitors) (A) and B-cell progenitors (B) in bone marrow from WT, *Btk* KO and BAC-transgenic mice. (A) CLPs (FLT3⁺IL7R⁺) are further subdivided based on LY6D to visualize the more B-cell specified LY6D⁺ CLPs. Right panel shows absolute number of indicated cell population per two femurs. (B) Sub-fractionation of CD19⁺ B-cells into Mature B (IgM⁺IgD⁺), Immature B (IgM⁺IgD⁻) and earlier progenitors based on BP1. Right panels show absolute number of indicated cell population per two femurs.



Supplemental Figure 6. Purity of pro-B cells. At the day of the transfection (day 9), the purity of the pro-B cells was assessed by CD19 staining and the viability of the cells was confirmed by PI staining. The purity and viability was checked for cells from duplicate animals with a representative result of each presented above.



Supplemental Figure 7. Restoration of BTK protein expression upon splice-correction after in vivo-treatment of BAC-transgenic mice. Western blot analysis of BTK restoration in two out of four treated animals; total cells from bone marrow and spleen (the other two treated animals are shown in Figure 8). Bar graph shows the quantitative analysis of BTK protein as percentage-relative intensity signal according to the ImageJ Software.